

EXPERIMENTAL REVIEW ON ω PRODUCTION

F.J. KLEIN

The Catholic University of America, Washington, DC 20064

P.L. COLE

*Jefferson Lab, Newport News, VA 23606 and
Idaho State University, Pocatello, ID 83209*

Over the past the three decades, the electro- and photoproduction of omega mesons have been studied predominantly with respect to diffractive and pion-exchange in the t channel. However, quark model calculations predict a significant coupling of the baryon resonances to the ωN channel, where many of the so-called missing baryon resonances are expected to couple strongly to both γN and ωN . But, due to the overall low cross section and the inherent difficulty in distinguishing N^* decay from t -channel processes, the ωN channel has not been thoroughly explored. With the advent of high-duty-cycle accelerators and large-acceptance detectors in the 1990s, ωp production is increasingly being investigated with respect to departures from diffraction-like behavior in the effort to extract s -channel contributions using electromagnetic probes.

MODEL CALCULATIONS

The first model calculations on ω production focused on t -channel exchange processes to describe the dominant features of the ω data available in the 1960s and 1970s. In the forward region, the Vector Meson Dominance (VDM) model provides an excellent description of the interaction of high-energetic (transverse) photons with matter. The incident photon dissociates into a virtual $q\bar{q}$ pair with $J^\pi=1^-$, which then scatters off the target nucleon. The photoproduction of ω s comes about through the isoscalar component in diffractive scattering, whereby the quantum numbers of the vacuum (Pomeron) are exchanged.^{1,2,3,4} However, when the virtual $q\bar{q}$ pair is an isovector state, a π^0 must be exchanged to allow for an ω meson to appear in the final state.⁵ The peripheral behavior of ωN production at low energies is well described by π^0 -exchange with a dressed $g_{\pi\omega\gamma}$ coupling for the dominant parity odd component (*unnatural parity*) and σ - or f_2 -exchange for the positive-parity (*natural-parity*) exchange.^{6,7,8} We note

that all models agree that pion-exchange dominates by far the ωN channel at low energies.

A comparatively good description of vector meson electro- and photo-production has been obtained by Y. Oh *et al.*⁸ This collaboration employs a Regge parameterization for Pomeron exchange⁹ as well as scalar (σ), pseudoscalar (π, η) and tensor (f_2)-exchange in the t channel and N -exchange in the u channel.

Above the resonance region, the model of J.-M. Laget^{7,10} affords even a better description of the photo- and electroproduction of ω s. He makes use of a two-gluon parameterization in Pomeron exchange with Reggeized pseudoscalar- and tensor-exchanges and N -exchange in the u channel.

SU(6) \otimes O(3) symmetric quark models predict a large variety of excited baryon states,^{11,12} of which most have not yet been experimentally confirmed or are still poorly established. These models predict comparatively large couplings of these resonances not only to the γN channel, but also to the ηN , $\Delta\pi$, ρN , and ωN channels as well. These latter channels are experimentally mostly *terra incognita*. Of particular interest are those channels which provide isospin selectivity, such as the ηN and the ωN reactions, since then only N^* s (and not the Δ^* s) may contribute in s -channel processes. Such selectivity greatly simplifies extracting the underlying resonant states.

In the relativized quark model of F. Close and Z.P. Li,¹³ the meson couples as point-like particle to the quark configuration in the baryon. Calculations based on this model by Z.P. Li and Q. Zhao^{14,15,16} predict considerable contributions to ωN from the subthreshold states $S_{11}(1535)$ and $D_{13}(1520)$. Near threshold, the dominant contributions arise from the $F_{15}(1680)$ and the $P_{13}(1720)$. At slightly higher energies, the $F_{15}(2000)$ plays an increasing role and – slightly suppressed – from $P_{13}(1900)$. The model incorporates π exchange – built-in in a consistent way – and Pomeron exchange based on Regge phenomenology. The model also includes the nucleon pole, the Roper, as well as seven other resonances in the SU(6) \otimes O(3) symmetry limit in s - and u -channel transitions through effective Lagrangians for the quark-photon and quark-vector-meson interactions.

The model of Y. Oh, A.I. Titov, and T-S.H. Lee⁸ employs $N^* \rightarrow \gamma N$ and $N^* \rightarrow \omega N$ amplitudes, where these amplitudes include configuration mixing effects due to quark-quark interactions. They explicitly include baryon resonances by incorporating Breit-Wigner descriptions and vertex functions provided by the relativized quark model of Capstick and Roberts.¹² Whereas for higher E_γ Pomeron exchange governs the total and differential

cross sections at low $|t|$, at lower energies pion exchange completely dominates the cross sections for the forward angles. This collaboration predicts that in the resonance region, the dominant contributions arise from the missing $P_{13}(1910)$ as well as the $D_{13}(1960)$ – which is identified with the PDG $D_{13}(2080)$ – and the $G_{17}(2190)$, with lesser contributions from the $F_{15}(2000)$. The inclusion of rescattering effects near threshold¹⁷ allows for describing the experimental data at threshold ($E_\gamma < 1.25$ GeV). Here, the dominant contributions are from the subthreshold resonance $D_{13}(1520)$ and the near-threshold resonance $F_{15}(1680)$.

EXPERIMENTAL RESULTS

Although the lightest two vector mesons, ρ and ω , have roughly the same mass of 770 MeV and 782 MeV, respectively, they possess very different decay widths,¹⁸ i.e. $\Gamma_\rho \sim 150$ MeV and $\Gamma_\omega = 8.4$ MeV. Without directly detecting the decay products, we cannot effectively distinguish these two vector mesons kinematically. At best one will only see a small ω peak situated on top of the broad ρ^0 spectrum obtained from the corresponding invariant or missing mass distributions. For a complete understanding of the dynamics, we require models that fit the distributions arising from these two vector mesons, which necessarily must include effects from ρ – ω mixing and the interference of ρ decay with the s -wave $\pi\pi$ -background.

With high-resolution and large-acceptance detectors, we may experimentally disentangle the ω from the ρ . By directly measuring the decay products in either the $\omega \rightarrow \pi^+\pi^-\pi^0$ (88.8%) and the $\omega \rightarrow \pi^0\gamma$ (8.5%) channels allows one to unambiguously distinguish the omega vector meson. But there remains the issue of the three-pion or the combinatoric three- γ background for statistically extracting the omega signal. Hence experiments with electromagnetic probes for ω production must rely on the detector's capability to resolve multiprong events.

Electroproduction experiments performed with two-arm spectrometers therefore face the difficulty of disentangling ρ and ω mesons.¹⁹ The recent electroproduction data near threshold at $Q^2=0.5$ GeV² were obtained using the high resolution spectrometers in Jefferson Lab's Hall C.²⁰ The ω yield was extracted by means of a maximum likelihood fit, which serves to account for the phase-space background in ρ^0 and ω production. In Fig.1 one sees a significant enhancement of backward production in the data. This behavior indicates large contributions from baryon exchange and is fully consistent with the Li-Zhao model (*solid curve*).

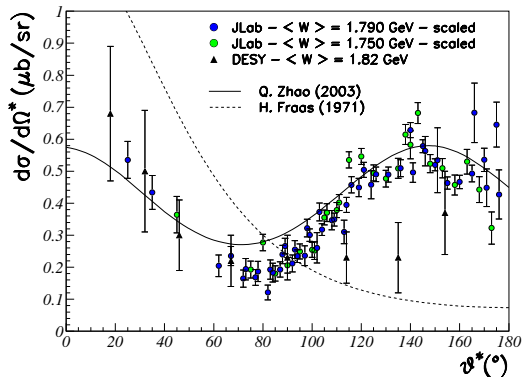


Figure 1. $ep \rightarrow e'p\omega$ data at $Q^2=0.5$ GeV^2 from Hall C (JLab): Angular distributions for different averaged W and for $|\phi^*| < 30^\circ$ in comparison to DESY data at $Q^2=0.77$ GeV^2 , $W=1.82$ GeV . The curves are from model calculations.^{5,16} This figure is from Ref.²⁰

Electroproduction data from CLAS, the large acceptance spectrometer in Hall B of Jefferson Lab, at $Q^2 > 0.5$ GeV^2 , covering the hadronic mass range from $W=1.75$ GeV to $W=2.20$ GeV are being analyzed, especially with regard to extraction of resonant contributions.²¹ The analysis of CLAS data at $Q^2 > 2.0$ GeV^2 , $W > 2.0$ GeV has recently been completed and will be ready for publication later this year.²² The preliminary data are presented in the lower two panels of Fig. 2. One sees that the Regge-based model of Laget¹⁰ reproduces the photoproduction data quite well. However, the electroproduction data show a considerable enhancement at large values of $|t|$, which can be accounted for by introducing a t dependence in the $\pi\omega\gamma$ form factor, thus suggesting a more point-like coupling at higher t .

Early experiments on photoproduction of ω used bubble-chamber detectors, and hence suffered from low statistics.^{24,25,26} They observed the dominant features of ω production: π^0 -exchange and at central production angles some departure from a characteristic exponential falloff in the differential cross section. A dip structure in the differential cross section around $u = -0.14$ GeV^2 was observed²⁷ in the backward angles for ω production for photon energies between 2.8 and 4.5 GeV . This structure can be described within the framework of Regge theory as N^α exchange.²⁸ The backward angle 1977 Daresbury data taken at 3.5 and 4.7 GeV are well reproduced via exchange in the u channel of the nucleon Regge trajectory.²⁹ Using a beam of linearly-polarized photons afforded by the Compton backscattering facility of SPring-8, the LEPS experiment has initiated new studies on the photoproduction of ω s at backward angles. However, since only the forward-going proton can be measured in the LEP detector, the ω extraction suffers from disentangling ω s from ρ^0 s within the multi-pion

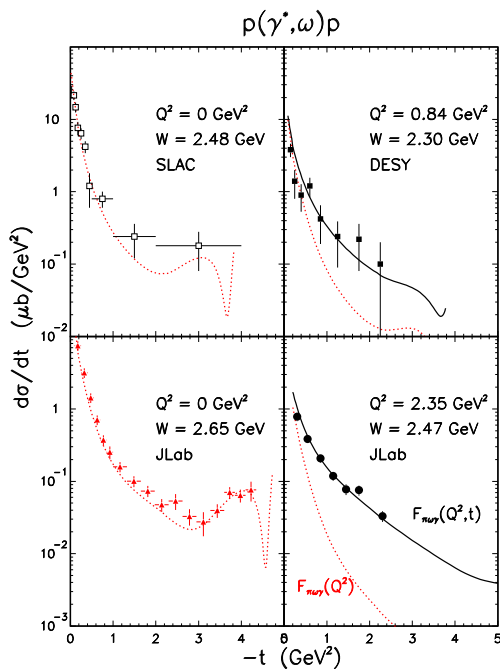


Figure 2. Differential cross section for ω photoproduction (*left panels*) and ω electroproduction (*right panels*) above the resonance regions ($W \approx 2.5$ GeV). Data points are from ³²(*upper left*), ¹⁹(*upper right*), ²³(*lower left*), ²²(*lower right*). The curves are from the Laget model:⁷ for the *dotted* curves the $\pi\omega\gamma$ form factor has only a Q^2 dependence, for the *solid* curves it has an additional t dependence.¹⁰ This figure is taken from Ref.²²

background.³⁰

Very few experiments up to now have made use of polarized photon beams. Linearly-polarized photon beams, for example, allow for separating the contributions from natural-parity (i.e. diffractive scattering) and unnatural-parity exchange (i.e. one-pion exchange) in the t -channel by analyzing the decay angular distribution arising from $\omega \rightarrow \pi^+\pi^-\pi^0$.³¹ The first experiment to exploit this parity filter feature was a SLAC experiment;³² they made use of backward Compton scattering to produce linearly polarized photons at 2.8, 4.7, and 9.3 GeV. The analysis of the ω decay distributions showed that the contribution of unnatural-parity exchange diminishes with increasing energy. This result was further confirmed by CERN experiments in the early 1980s which collected data on ω photoproduction at much higher photon energies.³³ At these higher energies – far above the resonance regime – these experiments show that the cross section and decay distributions can be explained purely in terms of VMD. The reaction proceeds almost entirely through natural-parity exchange in the t channel and is therefore s -channel helicity conserving, as is to expected from diffractive photoproduction. Other high energy ω production data taken at Cornell³⁴

and FNAL³⁵ confirm these results.

The GRAAL collaboration is studying ω photoproduction from threshold to $E_\gamma=1.5$ GeV. They employ a beam of linearly-polarized photons produced via Compton backscattering. By requiring a three-prong trigger and a reconstructed π^0 , the three-pion channel is well identified and the ω -peak is extracted via sideband subtraction. The resulting differential cross section shows large u -channel contributions and the extracted beam asymmetry Σ is strongly negative for $\theta^*(\omega) \approx 90^\circ$. Σ , however, approaches zero in the very forward and backward direction.³⁶ The authors of this paper are presently analyzing the photoproduction of ω s.³⁷ The linearly-polarized photon beam was produced with the coherent bremsstrahlung facility in Hall B of Jefferson Lab and the data were collected in the energy range of $1.8 < E_\gamma < 2.2$ GeV. Results are expected within a year.

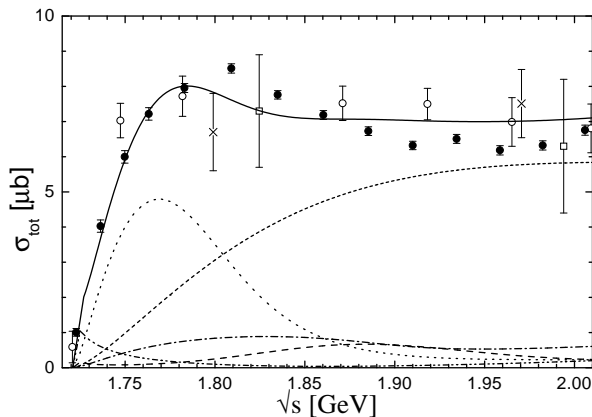


Figure 3. Total cross section for $\gamma p \rightarrow \omega p$: data from ³⁹(●), ⁴⁰(○), ²⁵(×), ²⁴(□) compared to coupled-channel fit results.³⁸ Figure taken from Ref.³⁹

New unpolarized photoproduction data have been taken at SAPHIR and CLAS. The final analysis of SAPHIR data at Bonn³⁹ comprises considerably larger statistics than previous data from SAPHIR.⁴⁰ The differential cross section (cf. Fig. 4) confirms the previously observed deviations from t -channel exchanges, especially near threshold where the angular distribution is almost flat. The new data resolve variations in the total cross section that have not been observed in earlier (low-statistics) results, particularly an excess at $W \approx 1.78$ – 1.81 GeV (cf. Fig. 3). The large set of data points allowed for integration of the ωN channel into a coupled-channel analysis.³⁸ The

partial-wave decomposition of the ωp cross section in Fig. 3 shows $P_{11}(1710)$ dominance near threshold (*dotted line*) and further non-negligible resonant contributions only in $J^\pi = \frac{3}{2}^+$, i.e. $P_{13}(1720)$ and $P_{13}(1900)$ (*dashed-dotted line*). π^0 exchange (*dashed line*) dominates the cross section behavior above $W \approx 1.82$ GeV.

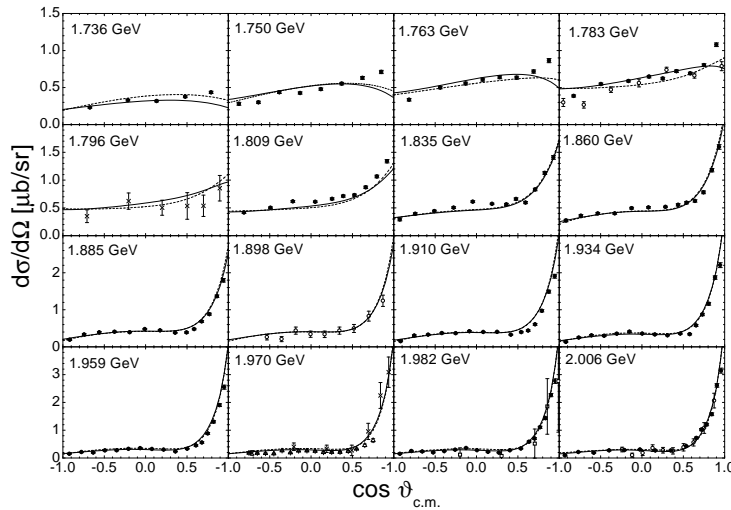


Figure 4. Differential cross section for $\gamma p \rightarrow \omega p$: data points and curves as in Fig. 3. The figure is taken from Ref.³⁹

The three-pion decay of ω allows for accessing the tensor polarization of this vector meson.^{31,41} The decay angular distributions of the SAPHIR data have been analyzed with regard to the spin density matrix elements (cf. Fig. 5). The extracted matrix elements confirm the earlier behavior observed in the differential cross section that the forward production is strongly dominated by π^0 -exchange, except at the near-threshold regime. In the intermediate and backward directions, there is a significant departure from what one would expect from t -channel exchange processes. Since these matrix elements are related to the off-diagonal polarization components, we are observing behavior not consistent with VDM or one-pion-exchange mechanisms. This analysis of the extraction of the density matrix elements, moreover, is in the resonance region and is unique. Earlier experiments on ω production were performed at higher energies, namely, at SLAC³² and CERN.³³ It is therefore imperative that this analysis be extended to en-

ergies in the resonance region with experiments employing polarized beam and/or polarized targets to provide the information necessary for delineating the individual processes which govern ωN production.

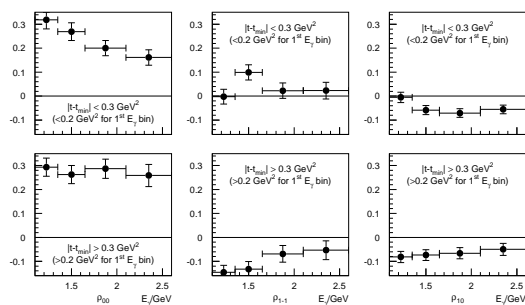


Figure 5. Spin density matrix elements in the helicity frame. The matrix elements were extracted from the ω decay distributions from the SAPHIR data.³⁹

The preliminary ω photoproduction data from CLAS⁴² show a very similar behavior. The decay distributions confirm the different behavior of ω production in forward and non-forward directions. The differential cross section has been extracted in photon energy bins of 50 MeV between $E_\gamma=1.15$ GeV to $E_\gamma=2.3$ GeV. Part of the data is presented in Fig. 6. The data has been compared to the Y.Oh model⁸ with Pomeron- and pion-exchange parameters adjusted to fit the published CLAS data at $E_\gamma=3.1-3.9$ GeV.²³ The *dotted* curve represents the contributions due to t -channel exchange processes, the *dashed* curve the resonant contribution – with couplings according to the relativized quark model,¹² and the *solid* curve the incoherent sum.

SUMMARY

There has been considerable theoretical and experimental progress in ω production with electromagnetic probes over the past several years. High statistics data have been – or are being – published, which offer the opportunity to investigate non-dominant contributions to the ωN channel. Experiments analyzing the decay angular distribution of $\omega \rightarrow \pi^+ \pi^- \pi^0$ as functions of the photon energy and the production angle (or four-momentum transfer squared) and experiments using polarized beams are poised to provide crucial information necessary for disentangling the various contributions in ω photo- and electroproduction.

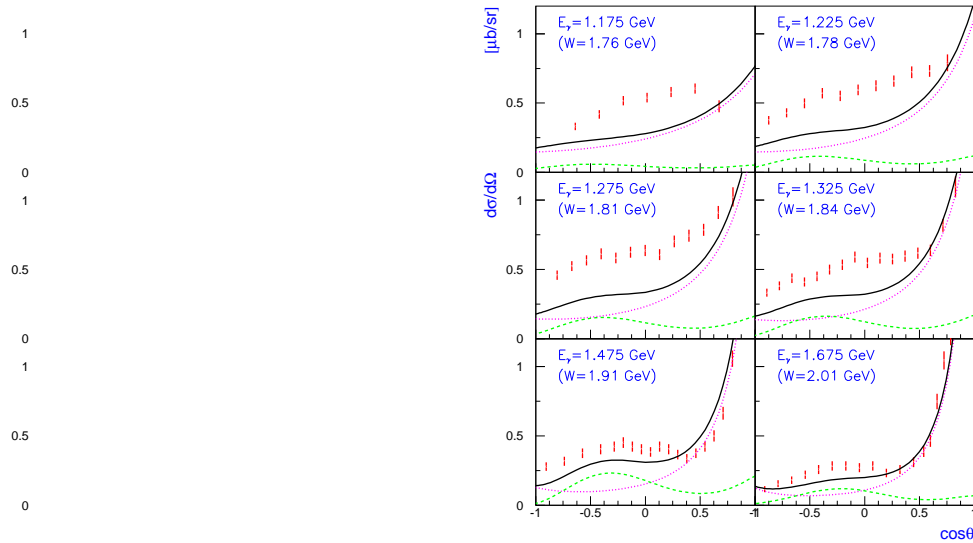


Figure 6. Preliminary CLAS data on ω photoproduction compared to the model of Y. Oh:⁸ Here, the *dotted* curve represents t -channel contributions, the *dashed* curve the resonant contributions, and the *solid* curve the incoherent sum.

Several models have been developed that describe not only the main features of ω production at low energies (π^0 -exchange) but also other t -channel exchange processes as well as resonant contributions in the s -channel. Theoretical predictions from all these models show that precise data on polarization observables are urgently needed to disentangle the various contributions.

We wish to thank the organizers of this conference for giving us this opportunity to present the experimental and theoretical progress in this interesting field of physics.

References

1. M. Ross and L. Stodolsky, Phys. Rev. **149** (1966) 1172.
2. N.M. Kroll, T.D. Lee, and B. Zumino, Phys. Rev. **157** (1967) 1376.
3. K. Schilling, in: Springer Tracks in Modern Physics 63 (1972) 31;
D. Schildknecht, *ibid.* 57.
4. A. Donnachie and G. Shaw, in: Photomagnetic Interactions of Hadrons, Vol.II, Plenum Press (1978) 169.
5. H. Fraas, Nucl. Phys. **B36** (1972) 191.

6. B.Friman and M.Soyeur, Nucl. Phys. **A600** (1996) 477.
7. J.-M. Laget, Phys. Lett. **B489** (2000) 313;
F. Cano and J.-M. Laget, Phys. Lett. **B551** (2003) 317.
8. Y. Oh, A. Titov, T.-S.H. Lee, Phys. Rev **C63** (2001) 025201;
Y. Oh and T.-S.H. Lee, Phys. Rev. **C66** (2002) 045201.
9. A. Donnachie and P.V. Landshoff, Nucl. Phys. **B244** (1984) 322.
10. J.-M. Laget, *work in progress*.
11. N. Isgur and G. Karl, Phys. Lett. **B72** (1977) 109;
N. Isgur and R. Koniuk, Phys. Rev. **D21** (1980) 1868.
12. S. Capstick, Phys. Rev. **D46** (1992) 2864;
S. Capstick and W. Roberts, Phys. Rev. **D49** (1994) 4570.
13. F.E. Close and Z.P. Li, Phys. Rev. **D42** D (1990) 2194;
Phys. Rev **D42** (1990) 2207.
14. Q. Zhao, Z.P. Li, C. Bennhold, Phys. Lett. **B436** (1998) 42;
Phys. Rev **C58** (1998) 2393.
15. Q. Zhao, Phys. Rev **C63** (2001) 025203.
16. Q. Zhao, *work in progress*.
17. A. Titov and T.-S.H. Lee, Phys. Rev **C66** (2002) 015204.
18. Review of Particle Physics, Eur. Phys. J. **C15** (2000).
19. P. Joos *et al.*, Nucl. Phys. **B113** (1976) 53; Nucl. Phys. **B122** (1977) 365.
20. P. Ambrozewicz *et al.*, arXiv:nucl-ex/0403003.
21. F.J. Klein *et al.*, Proc. BARYONS2002, World Scient. (2003) 489.
22. L. Morand, Ph.D. thesis, U. Paris 7 (12/2003).
23. M. Battaglieri *et al.*, Phys. Rev. Lett. **90** (2003) 022002.
24. H.R. Crouch *et al.*, Phys. Rev. **155** (1967) 1468.
25. R. Erbe *et al.*, Phys. Rev. **175** (1968) 1669.
26. Y. Eisenberg *et al.*, Phys. Rev. Lett. **22** (1969) 669.
27. R.L. Anderson *et al.*, Phys. Rev. **D12** (1976) 679; R.W. Clift *et al.*, Phys. Lett. **B72** (1977) 144; D.P. Barber *et al.*, Z. Phys. **C26** (1984) 343.
28. Dainton, Lecture Notes in Physics **234** (1984) 80.
29. F. Cano and J.M. Laget, Phys. Rev. **D65** (2002) 074022; J.M. Laget, Proc. *Exclusive Processes at High Momentum Transfer*, World Scient. (2002) 44.
30. T. Hotta *et al.*, Nucl. Phys. **A721** (2003) 751c.
31. K. Schilling, P. Seyboth, G. Wolf, Nucl. Phys.**B15** (1970) 397.
32. J. Ballam *et al.*, Phys. Rev. **D7** (1973) 3150.
33. Atkinson *et al.*, Nucl. Phys. **B231** (1984) 15.
34. J. Abramson *et al.*, Phys. Rev. Lett. **36** (1976) 1428.
35. J. Busenitz *et al.*, Phys. Rev. **D40** (1089) 1.
36. E. Hourany *et al.*, Proc. NSTAR2002, World Scient. (2003) 261.
37. F.J. Klein and P.L. Cole, cospokespersons, JLab Experiment E-99-013.
38. G. Penner and U. Mosel, Phys. Rev. **C66** (2002) 055212.
39. J. Barth *et al.*, Eur. Phys. J. **A18** (2003) 117.
40. F.J. Klein *et al.*, πN Newsletters **14** (1998) 141.
41. C. Savkli, F. Tabakin, S.N. Yang, Phys. Rev. **C53** (1996) 1132.
42. F.J. Klein, *work in progress*.